1 **Disruption of the CCL5/RANTES-CCR5 Pathway Restores Immune**

2 **Homeostasis and Reduces Plasma Viral Load in Critical COVID-19**

3

4 Bruce K. Patterson[1,^], Harish Seethamraju[2], Kush Dhody[3], Michael J. Corley[4], Kazem

5 Kazempour[3], Jay Lalezari[5], Alina P.S. Pang[6], Christopher Sugai[6], Edgar B. Francisco[1],

6 Amruta Pise[1], Hallison Rodrigues[1], Mathew Ryou[1], Helen L. Wu[7], Gabriela M. Webb[7],

7 Byung S. Park[7], Scott Kelly[8], Nader Pourhassan[8], Alena Lelic[9], Lama Kdouh[9], Monica

8 Herrera[10], Eric Hall[10], Enver Aklin[2], Lishomwa C. Ndhlovu[4*], Jonah B. Sacha[7*]

9

10 [1]IncellDX, Menlo Park, CA, USA, [2]Montefiore Medical Center, New York, NY, USA,

11 [3]Amarex Clinical Research LLC, Germantown, MD, USA, [4]Division of Infectious

12 Diseases, Department of Medicine, Weill Cornell Medicine, New York, NY, USA, [5]Quest

13 Clinical Research, San Francisco, California, USA, [6]University of Hawaii, Honolulu, HI,

14 USA, [7]Vaccine & Gene Therapy Institute, Oregon Health & Science University, Portland,

15 OR, USA, [8]CytoDyn Inc., Vancouver, WA, USA, [9]Beckman Coulter, Miami, FL, USA,

16 [10]Bio-Rad, Pleasanton, CA, USA.

17

18 *Co-senior authors

19
20 ^Corresponding author:
21 Bruce K. Patterson, MD
22 IncellDx, Inc
23 1541 Industrial Road
24 San Carlos, CA 94070
25 Tel: +1.650.777.7630
26 Fax: +1.650.587.1528
27 brucep@incelldx.com

ABSTRACT

Severe acute respiratory syndrome coronavirus 2 (SARS-CoV-2), the causative agent of coronavirus disease 2019 (COVID-19), is now pandemic with nearly three million cases reported to date[1]. Although the majority of COVID-19 patients experience only mild or moderate symptoms, a subset will progress to severe disease with pneumonia and acute respiratory distress syndrome (ARDS) requiring mechanical ventilation[2]. Emerging results indicate a dysregulated immune response characterized by runaway inflammation, including cytokine release syndrome (CRS), as the major driver of pathology in severe COVID-19[3,4]. With no treatments currently approved for COVID-19, therapeutics to prevent or treat the excessive inflammation in severe disease caused by SARS-CoV-2 infection are urgently needed. Here, in 10 terminally-ill, critical COVID-19 patients we report profound elevation of plasma IL-6 and CCL5 (RANTES), decreased CD8+ T cell levels, and SARS-CoV-2 plasma viremia. Following compassionate care treatment with the CCR5 blocking antibody leronlimab, we observed complete CCR5 receptor occupancy on macrophage and T cells, rapid reduction of plasma IL-6, restoration of the CD4/CD8 ratio, and a significant decrease in SARS-CoV-2 plasma viremia. Consistent with reduction of plasma IL-6, single-cell RNA-sequencing revealed declines in transcriptomic myeloid cell clusters expressing IL-6 and interferon-related genes. These results demonstrate a novel approach to resolving unchecked inflammation, restoring immunologic deficiencies, and reducing SARS-CoV-2 plasma viral load via disruption of the CCL5-CCR5 axis, and support randomized clinical trials to assess clinical efficacy of leronlimab-mediated inhibition of CCR5 for COVID-19.

MAIN TEXT

Since the initial cases of COVID-19 were reported from Wuhan, China in December 2019[2], SARS-CoV-2 has emerged as a global pandemic with an ever-increasing number of severe cases requiring invasive external ventilation that threatens to overwhelm health care systems[1]. While it remains unclear why COVID-19 patients experience a spectrum of clinical outcomes ranging from asymptomatic to severe disease, the salient features of COVID-19 pathogenesis and mortality are rampant inflammation and CRS leading to ARDS[4,5]. Indeed, excessive immune cell infiltration into the lung, cytokine storm, and ARDS have previously been described as defining features of severe disease in humans infected with the closely related betacoronaviruses SARS-CoV and MERS-CoV[6,7]. Because SARS-CoV-infected airway epithelial cells and macrophages express high levels of CCL5[8,9], a chemotactic molecule able to amplify inflammatory responses towards immunopathology, we hypothesized that disrupting the CCL5-CCR5 axis via leronlimab-mediated CCR5 blockade would prevent pulmonary trafficking of pro-inflammatory leukocytes and reverse cytokine storm in COVID-19.

Leronlimab, formerly PRO 140, is a CCR5-specific human IgG4 monoclonal antibody in development for HIV therapy as a once-weekly, at-home subcutaneous injection. In five completed and four ongoing HIV clinical trials where over 800 individuals have received leronlimab, no drug related deaths, serious injection site reactions, or drug-drug interactions were reported[10-13]. Self-administration of leronlimab by patients facilitates simple, once-weekly dosing. In contrast to the small molecule CCR5 inhibitors that prevent HIV Env binding to CCR5 via allosteric modulation, leronlimab binds to the CCR5

3

75 extracellular loop 2 domain and N-terminus, thereby directly blocking the binding of HIV

76 Env to the CCR5 co-receptor via a competitive mechanism. Leronlimab does not

77 downregulate CCR5 surface expression or deplete CCR5-expressing cells, but does

78 prevent CCL5-induced calcium mobilization in CCR5+ cells with an IC_{50} of 45 μg/ml[14].

79 This ability to specifically prevent CCL5-induced activation and chemotaxis of

80 inflammatory CCR5+ macrophages and T cells suggests that leronlimab might be

81 effective in resolving pathologies involving the CCL5-CCR5 pathway.

82

83 Ten critical COVID-19 patients at the Montefiore Medical Center received leronlimab via

84 FDA-approved emergency investigational new drug (EIND) requests for individual patient

85 use (Table 1). These confirmed SARS-CoV-2 positive patients had significant pre-existing

86 co-morbidities and were receiving intensive care treatment including mechanical

87 ventilation or supplemental oxygen for ARDS. Consistent with previous reports of severe

88 COVID-19 disease[2], these patients showed evidence of lymphopenia with liver and

89 kidney damage (Supplementary Fig. 1)[15]. Four of the patients died during the fourteen-

90 day study period due to a combination of disease complications and severe constraints

91 on medical equipment culminating in medical triage. Although this EIND study lacks a

92 placebo control group for comparison, a recent study of other critically ill COVID-19

93 patients in the New York City area indicates mortality rates as high as 88%[16].

94

95 Hyper immune activation and cytokine storm are present in cases of severe COVID-19[4].

96 Indeed, at leronlimab treatment baseline, signatures of CRS were present in the plasma

97 of all ten patients in the form of significantly elevated levels of the inflammatory cytokines

4

98   IL-1β, IL-6, and IL-8 (Fig. 1a-c) compared to healthy controls. In comparison to patients

99   with mild or moderate COVID-19, only IL-6 was present at significantly higher levels in

100   critically-ill patients. Of note, plasma CCL5 levels in the ten critically ill patients were

101   markedly elevated over those in both healthy controls and mild or moderate COVID-19

102   patients (Fig. 1d). High levels of CCL5 can cause acute renal failure and liver toxicity[17,18],

103   both common findings in COVID-19 infection. Indeed, the critically ill patients presented

104   with varying degrees of kidney and liver injury, although many had also previously

105   received kidney transplants[15] (Table 1 and Supplementary Fig. 1).

106

107   At study day zero, all ten critically ill patients received a subcutaneous 700mg injection of

108   leronlimab following baseline blood collection. Because defining features of severe

109   COVID-19 disease include plasma IL-6 and T cell lymphopenia[2,19], and we observed

110   >100-fold increased CCL5 levels compared to normal controls (Fig. 1d), we longitudinally

111   monitored these parameters for two weeks after leronlimab treatment. A reduction of

112   plasma IL-6 was observed as early as three days following leronlimab and returned to

113   healthy control levels by day 14 (Fig. 2a). In contrast, more variable levels were observed

114   with IL-1β, IL-8, and CCL5 after leronlimab treatment (Supplementary Fig. 2). Following

115   leronlimab administration, a marked restoration of CD8+ T cells (Fig. 2b) and a

116   normalization of the CD4+ and CD8+ T cell ratio in blood was observed (Fig. 2c). These

117   immunological changes occurred concomitant with full leronlimab CCR5 receptor

118   occupancy on the surface of CCR5+ T cells and macrophages (Fig. 2d, 2e). Low levels

119   of SARS-CoV-2 have been detected, but not yet quantified in the plasma of COVID-19

120   patients[19]. We used high sensitivity, digital droplet PCR to quantify plasma SARS-CoV-2

121   viremia at baseline. SARS-CoV-2 was found in the plasma of all ten critically ill patients,

122   underscoring the severity of COVID-19 (Fig. 2f). Following leronlimab administration

123   SARS-CoV-2 plasma viremia decreased in all patients at day seven, suggesting more

124   effective anti-viral immunity following leronlimab-mediated CCR5 blockade.

125

126   Finally, to establish an unbiased gene repertoire for these COVID-19 patients, we

127   performed 10X Genomics 5' single cell RNA-sequencing of peripheral blood mononuclear

128   cells to evaluate transcriptional changes between an uninfected healthy donor and two of

129   the severe COVID-19 patients (P2 and P4) for which sufficient baseline, pre-leronlimab

130   treatment COVID-19 samples were available for this analysis. We identified 2,890

131   differentially expressed transcripts between the two groups and found that the two severe

132   COVID-19 patients had a greater abundance of myeloid cells upregulating inflammatory-

133   , interferon (IFN)-, and chemokine-related genes compared to a healthy control (FDR <

134   0.05) (Supplementary Table 2). Notable genes overexpressed in COVID-19 samples

135   included chemokines (CXCL8, CCL4, CCL3), inflammatory and immune activation genes

136   (IL-1b, CD69), and the IFN-related genes (IFI27, IFITM3) (Supplementary Fig. 3). We

137   also observed a downregulation of the effector molecule granzyme A and the

138   immunoregulatory gene KLRB1 compared to the healthy control.

139

140   To identify markers that would inform effective leronlimab treatment we conducted

141   differential expression analysis for the same two severe COVID-19 participants (P2 and

142   P4) for which baseline and day seven post leronlimab samples were available. Our

143   longitudinal COVID-19 single cell dataset profiled an estimated 4,105 cells at baseline

144   and 4,888 cells at the 7-day post leronlimab timepoint. We identified 2,037 differentially

145   expressed transcripts (FDR < 0.05) (Supplementary Table 2). In line with the decrease of

146   IL-6 protein levels observed in plasma, IL-6 transcripts were downregulated between day

147   0 and day 7 in monocytes, (Supplementary Fig. 4), consistent with reports of

148   monocyte/macrophages repolarization following CCR5 blockade[20]. We observed that

149   myeloid cells expressing chemokine and IFN-related genes such as CCL3, CCL4, CCL5,

150   ADAR, APOBEC3A, IFI44L, ISG15, MX1 were downregulated at day 7 post leronlimab

151   compared to baseline (Fig. 3 and Supplementary Table 3). Within the T cell population,

152   we observed increased expression of granzyme A, suggesting improved antiviral function.

153   These transcriptomic findings further underscore the potential impact of leronlimab-

154   mediated CCR5 blockade on the inflammatory state in COVID-19.

155

156   Here, we report on the involvement of the CCL5-CCR5 pathway in COVID-19 and present

157   data from ten critically ill patients with severe COVID-19 demonstrating reduction of

158   inflammation, restoration of T cell lymphocytopenia, and reduced SARS-CoV-2 plasma

159   viremia following leronlimab-mediated CCR5 blockade. Recent studies have found that a

160   significant number of COVID-19 patients experience increased risks of strokes, blood

161   clots and other thromboembolic events[21]. Platelet activation, which leads to the initiation

162   of the coagulation cascade, can be triggered by chemokines including CCL5[22],

163   suggesting that leronlimab treatment may be beneficial beyond its immunomodulatory

164   effects on inflammation and hemostasis in COVID-19 patients.

165

166 Given medical triage resulting in patient death, we cannot comment on the impact of

167 leronlimab on clinical outcome in these patients. While anecdotal evidence of clinical

168 improvement in COVID-19 patients following leronlimab treatment have been reported[23],

169 randomized controlled trials are required to determine efficacy of leronlimab for COVID-

170 19. Indeed, randomized, double blind, placebo controlled clinical trials are underway to

171 assess the efficacy of leronlimab treatments in patients with mild to moderate

172 (NCT04343651)[24] and severe to critical (NCT04347239)[25] COVID-19. In summary, we

173 show here for the first time, involvement of the CCL5-CCR5 axis in the pathology of

174 SARS-CoV-2, and present evidence that inhibition of CCL5 activity via CCR5 blockade

175 represents a novel therapeutic strategy for COVID-19 with both immunologic and virologic

176 implications.

177

178 **METHODS**

179 <u>Assessment of plasma cytokine and chemokine levels.</u>

180 Fresh plasma was used for cytokine quantification using a customized 13-plex bead-

181 based flow cytometric assay (LegendPlex, Biolegend, Inc) on a CytoFlex flow cytometer.

182 For each patient sample 25 µL of plasma was used in each well of a 96-well plate. Raw

183 data was analyzed using LegendPlex software (Biolegend, Inc San Diego CA). Samples

184 were run in duplicate. In addition, split sample confirmation testing was performed by

185 ELISA (MDBiosciences, Minneapolis, MN). A 48-plex cytokine/chemokine/growth factor

186 panel and RANTES-CCL5 (Millipore Sigma) assay were performed following

187 manufacture's protocol on a Luminex MAGPIX instrument. Confirmation testing was also

188 performed in duplicate. Samples falling outside the linear range of the appropriate

189   standard curves were diluted and repeated incorporating the dilution factor into the final

190   average. Cytokine, chemokines and growth factors included: sCD40L, EGF, Eotaxin,

191   FGF-2, Flt-3, Fractalkine, G-CSF, GM-CSF, GRO-α, IFNα2, IFNγ, IL-1α, IL-1β, IL-1ra, IL-

192   2, IL-3, Il-4, IL-5, IL-5, IL-6, IL-7, IL-8, IL-9, IL-10, IL-12 (p40), IL-12 (p70), IL-13, IL-15,

193   IL-17A, IL-17E/IL-25, IL-17F, IL-18, IL-22, IL-27, IP-10, MCP-1, MCP-3, M-CSF, MDC,

194   MIG, MIP-1α, MIP-1β, PDGF-AA, PDGF-AB/BB, RANTES, TGF-α, TNF-α, TNF-β, and

195   VEGF.

196

197   Flow cytometry.

198   Peripheral blood mononuclear cells were isolated from peripheral blood using

199   Lymphoprep density gradient (STEMCELL Technologies, Vancouver, Canada). Aliquots

200   of cells were frozen in media that contained 90% fetal bovine serum (HyClone, Logan,

201   UT) and 10% dimethyl sulfoxide (Sigma-Aldrich, St. Louis, MO) and stored at -70C. Cells

202   were quick thawed, washed, and incubated with 2% solution of bovine serum albumin

203   (Blocker BSA, ThermoFisher, Waltham, MA) diluted in D-PBS (HyClone) for 5 min. Each

204   sample received a cocktail containing 10 uL Brilliant Stain Buffer (BD Biosciences,

205   Franklin Lakes, NJ), 5 uL True-Stain Monocyte Blocker (BioLegend, San Diego, CA), and

206   the following surface marker antibodies: anti-CD19 (PE-Dazzle594), anti-CD3 (APC),

207   anti-CD16 (Alexa700), HLA-DR (APC/Fire750), and anti-CTLA-4 (PE-Cy7). The following

208   antibodies were then added to each tube individually: anti-CD8 (BUV496), anti-

209   CD4 (BUV661), anti-CD45 (BUV805), anti-CD103 (BV421), anti-TIM3 (BV605), anti-

210   CD56 (BV650), anti-LAG-3 (BV711), anti-CD14 (BB785), and anti-PD-1 (BB700),

211   followed by a 30 min. incubation in the dark at room temperature. Cells were washed

9

212   once with 2% BSA solution before fixation and permeabilization. Cells were fixed and

213   permeabilized in a one-step reaction with 1X incellMAX (IncellDx, San Carlos, CA) at a

214   concentration of 1 million cells per mL and incubated for 60 min. in the dark at room

215   temperature. Cells were washed once with 2% BSA solution, and analyzed on a Cytoflex

216   LX with 355nm (20mW), 405nm (80mW), 488nm (50mW), 561nm (30mW), 638nm

217   (50mW), 808nm (60mW) lasers (Beckman Coulter Life Sciences, Indianapolis, IN).

218   Analysis was performed with Kaluza version 2.1 software. The panel used in this study is

219   shown in Supplementary Table 1 and examples of the gating strategy is shown in

220   Supplementary Fig. 5.

221

222   CCR5 receptor occupancy.

223   Because CCR5 is a highly regulated receptor especially in infection, inflammation, and

224   cancer, we determined CCR5 receptor occupancy by leronlimab by using phycoerythrin-

225   labeled leronlimab (IncellDx, Inc) in a competitive flow cytometry assay. CCR5-

226   expressing immune cells including CD4+, CD45RO+ T-lymphocytes, CD4+, FoxP3+ T-

227   regulatory cells, and CD14+, CD16+ monocytes/macrophages were included in the panel

228   using the appropriate immunophenotypic markers for each population in addition to PE-

229   labeled leronlimab. Cells were incubated for 30 min. in the dark at room temperature

230   and washed twice with 2% BSA solution before flow acquisition on a 3-laser CytoFLEX

231   fitted with 405nm (80mW), 488nm (50mW), 638nm (50mW) lasers (Beckman Coulter Life

232   Sciences, Indianapolis, IN Life Sciences, Indianapolis, IN). Receptor occupancy was

233   determined by the loss of CCR5 detection over time in these subpopulations

234   (Supplementary Figure 6) and calculated with the following equation:

235   1-A/B X 100 where A is Day 0 and B is Day 7.

236

237   <u>Measurement of plasma SARS-CoV-2 viral loads.</u>

238   The QIAamp Viral Mini Kit (Qiagen, Catalog #52906) was used to extract nucleic acids

239   from 300-400 µL from plasma sample according to instructions from the manufacturer

240   and eluted in 50 µL of AVE buffer (RNase-free water with 0.04% sodium azide). The

241   purified nucleic acids were used immediately with the Bio-Rad SARS-CoV-2 ddPCR Kit

242   (Bio-Rad, Hercules, CA). Each batch of samples extracted comprised positive and

243   extraction controls which are included in the kit, as well as a no template control (nuclease

244   free water). The Bio-Rad SARS-CoV-2 ddPCR Test is a reverse transcription (RT) droplet

245   digital polymerase chain reaction (ddPCR) test designed to detect RNA from SARS-CoV-

246   2. The oligonucleotide primers and probes for detection of SARS-CoV-2 are the same as

247   those reported by CDC and were selected from regions of the viral nucleocapsid (N) gene.

248   The panel is designed for specific detection of the 2019-nCoV (two primer/probe sets).

249   An additional primer/probe set to detect the human RNase P gene (RP) in control samples

250   and clinical specimens is also included in the panel as an internal control. The Bio-Rad

251   SARS-CoV-2 ddPCR Kit includes these three sets of primers/probes into a single assay

252   multiplex to enable a one-well reaction. RNA isolated and purified from the plasma

253   samples (5.5 µL) were added to the mastermix comprised of 1.1 µL of 2019-nCoV triplex

254   assay, 2.2 µL of reverse transcriptase, 5.5 µL of supermix, 1.1 µL of Dithiothreitol (DTT)

255   and 6.6 µL of nuclease-free water. Twenty-two microliters (22µl) from these sample and

256   mastermix RT-ddPCR mixtures were loaded into the wells of a 96-well PCR plate. The

257   mixtures were then fractionated into up to 20,000 nanoliter-sized droplets in the form of a

258   water-in-oil emulsion in the QX200 Automated Droplet Generator (Bio-Rad, Hercules CA).

259   The 96-well RT-ddPCR ready plate containing droplets was sealed with foil using a plate

260   sealer and thermocycled to achieve reverse transcription of RNA followed by PCR

261   amplification of cDNA in a C1000 Touch thermocycler (Bio-Rad, Hercules CA).

262   Subsequent to PCR, the plate was loaded into the QX200 Droplet Reader (Bio-Rad,

263   Hercules CA) and the fluorescence intensity of each droplet was measured in two

264   channels (FAM and HEX). The Droplet Reader singulates the droplets and flows them

265   past a two-color fluorescence detector. The detector reads the droplets to determine

266   which contain target (positive) and which do not (negative) for each of the targets

267   identified with the Bio-Rad SARS-CoV-2 ddPCR Test: N1, N2 and RP. The fluorescence

268   data is then analyzed by the QuantaSoft 1.7 and QuantaSoft Analysis Pro 1.0 Software

269   to determine the presence of SARS-CoV-2 N1 and N2 in the specimen.

270   **Bio-Rad SARS-CoV-2 RT-ddPCR Thermal Cycling Protocol**

Cycling Step	Temperature (ºC)	Time	Number of Cycles
Reverse Transcription	50	60 minutes	1
PCR enzyme activation	95	10 minutes	1
Template Denaturation	94	30 seconds	40
Annealing / Extension	55	60 seconds	

Droplet Stabilization	4	30 minutes	1
Hold (optional)	4	Overnight	1

271

272

273 Statistical Analysis.

274 The inflammatory cytokines IL-1β, IL-6, IL-8, CCL5 levels between groups were compared

275 using non-parametric Kruskal-Wallis test followed by Dunn's multiple comparison

276 correction to control the experimental wise error rate. To assess reversal of immune

277 dysfunction and CCR5 receptor occupancy as well as cytokine and chemokine levels in

278 severe COVID-19 patients after Leronlimab, Kruskal-Wallis test with Dunn's multiple

279 comparison correction was used. Changes in SARS-CoV-2 plasma viral loads were

280 assessed using the Mann-Whitney test.

281

282 Patient samples and IRB.

283 All patients were enrolled in this study under an individual patient emergency use

284 investigation new drug (EIND) via FDA emergency use authorization (EUA). The FDA

285 assigned an EIND number for each patient and thus registration in a clinical trial

286 registration agency is not applicable. Informed consent was obtained from patient or their

287 legally authorized representative per 21 CFR Part 50. The Albert Einstein College of

288 Medicine Institution Review Board (IRB) reviewed and approved this study. The IRB was

289 notified within 5 business days of treatment initiation. Within 15 business days of FDA

290 emergency use authorization, Form FDA 3926 along with the treatment plan and the letter

291 of authorization from CytoDyn was submitted to FDA. One 8 mL EDTA tube and one 4

292   mL plasma preparation (PPT) tube were drawn by venipuncture at Day0 (pre-treatment),

293   Day 3, Day 7, Day 14 post-treatment. Blood was shipped overnight to IncellDX for

294   processing and analysis. Peripheral blood mononuclear cells were isolated from

295   peripheral blood using Lymphoprep density gradient (STEMCELL Technologies,

296   Vancouver, Canada). Aliquots of cells were frozen in media that contained 90% fetal

297   bovine serum (HyClone, Logan, UT) and 10% dimethyl sulfoxide (Sigma-Aldrich, St.

298   Louis, MO) and stored at -70C.

299

300   10X Genomics 5' Single-cell RNA-Sequencing

301   Cryopreserved PBMC cells were thawed in RMPI 1640 complete medium, washed in PBS

302   BSA 0.5%, and cell number and viability measured using a Countess II automated cell

303   counter (Thermo Fisher Scientific). Cells were then diluted to a concentration of 1 million

304   cells per ml for loading into the 10X chip. Single-cell RNA-Sequencing library preparation

305   occurred with the Chromium Next GEM Single Cell Immune Profiling (v.1.1 Chemistry)

306   according to manufacturer's protocols on a Chromium Controller instrument. The library

307   was sequenced using a High Output Flowcell and Illumina NextSeq 500 instrument. For

308   data processing, Cellranger (v.3.0.2) mkfastq was applied to the Illumina BCL output to

309   produce FASTQ files. Cellranger count was then applied to each FASTQ file to produce

310   a feature barcoding and gene expression matrix. Cellranger aggr was used to combine

311   samples for merged analysis. For quality control, we applied the *Seurat* package for cell

312   clustering and differential expression analyses.

313

314   **ACKNOWLEDGMENTS**

14

321

322   AUTHOR CONTRIBUTIONS

323   BKP, HS, KD, KK, JL, SK, NP, JBS conceived of the study, HS and EA coordinated

324   patient care, BKP, HS, AP, EBF, HR, WR, AL, LK, MH, and EH acquired data, BKP, MJC,

325   APSP, CS, BF, HLW, GMW, BSP, SK, JL, AL, LK, MH, EH, LCN, and NP analyzed data,

326   and BKP, MJC, KD, JL, HLW, GMW, BSO, SK, NP, LCN, and JBS wrote the manuscript.

327

328   DATA AVAILABILITY

329   All primary data presented in this study are available from the corresponding author upon

330   reasonable request. Primary data exists for all figures.

331

332   COMPETING INTERESTS

333   Dr. Sacha has received compensation for consulting for CytoDyn Inc., a company that

334   may have a commercial interest in the results of this research. The potential conflict of

335   interest has been reviewed and managed by Oregon Health & Science University. Drs.

336   Kelly and Pourhassan are employees of CytoDyn Inc., owner and developer of

337   Leronlimab. Dr. Lalezari is a principal investigator for CytoDyn Inc. through his company

338 Quest Clinical Research. Dr. Patterson, Brian Francisco, Amruta Pise, Matthew Ryou,

339 Hallison Rodrigues are employees of IncellDx, Inc., a diagnostic company providing

340 assays to Cytodyn Inc. Dr. Ndhlovu has received compensation for serving on a scientific

341 advisory board for Abbvie. Lama Kdouh and Alina Lelic are employees of Beckman

342 Coulter Life Sciences, and Monica Herrera and Eric Hall are employees of Bio-Rad,

343 Inc. Drs. Kush Dhody and Kazem Kazempour are employees of Amarex Clinical

344 Research, LLC, a company that manages clinical trials and regulatory matters for

345 CytoDyn Inc.

346

347 **REFERENCES**

348

349 1.   World Health Organization. Coronavirus disease (COVID-2019) situation reports.

350   https://www.who.int/emergencies/diseases/novel-coronavirus-2019/situation-

351   reports.

352 2.   Huang, C. *et al.* Clinical features of patients infected with 2019 novel coronavirus

353   in Wuhan, China. *Lancet* **395,** 497–506 (2020).

354 3.   Zhang, D. *et al.* COVID-19 infection induces readily detectable morphological and

355   inflammation-related phenotypic changes in peripheral blood monocytes, the

356   severity of which correlate with patient outcome. *medRxiv* 2020.03.24.20042655

357   (2020). doi:10.1101/2020.03.24.20042655

358 4.   Mehta, P. *et al.* COVID-19: consider cytokine storm syndromes and

359   immunosuppression. *Lancet* **395,** 1033–1034 (2020).

16

360   5.   Qin, C. *et al.* Dysregulation of immune response in patients with COVID-19 in

361   Wuhan, China. *Clin. Infect. Dis.* (2020). doi:10.1093/cid/ciaa248

362   6.   Channappanavar, R. & Perlman, S. Pathogenic human coronavirus infections:

363   causes and consequences of cytokine storm and immunopathology. *Semin*

364   *Immunopathol* **39,** 529–539 (2017).

365   7.   Nicholls, J. M. *et al.* Lung pathology of fatal severe acute respiratory syndrome.

366   *Lancet* **361,** 1773–1778 (2003).

367   8.   Law, H. K. W. *et al.* Chemokine up-regulation in SARS-coronavirus-infected,

368   monocyte-derived human dendritic cells. *Blood* **106,** 2366–2374 (2005).

369   9.   Yen, Y.-T. *et al.* Modeling the early events of severe acute respiratory syndrome

370   coronavirus infection in vitro. *Journal of Virology* **80,** 2684–2693 (2006).

371   10. Jacobson, J. M. *et al.* Antiviral activity of single-dose PRO 140, a CCR5 monoclonal

372   antibody, in HIV-infected adults. *J. Infect. Dis.* **198,** 1345–1352 (2008).

373   11. Jacobson, J. M. *et al.* Anti-HIV-1 activity of weekly or biweekly treatment with

374   subcutaneous PRO 140, a CCR5 monoclonal antibody. *J. Infect. Dis.* **201,** 1481–

375   1487 (2010).

376   12. Jacobson, J. M. *et al.* Phase 2a study of the CCR5 monoclonal antibody PRO 140

377   administered intravenously to HIV-infected adults. *Antimicrob. Agents Chemother.*

378   **54,** 4137–4142 (2010).

379   13. Dhody, K. *et al.* PRO 140, a monoclonal antibody targeting CCR5, as a long-acting,

380   single-agent maintenance therapy for HIV-1 infection. *HIV Clin Trials* **19,** 85–93

381   (2018).

382   14.   Olson, W. C. *et al.* Differential inhibition of human immunodeficiency virus type 1 fusion, gp120 binding, and CC-chemokine activity by monoclonal antibodies to CCR5. *Journal of Virology* **73,** 4145–4155 (1999).

385   15.   Akalin, E. *et al.* Covid-19 and Kidney Transplantation. *N Engl J Med* NEJMc2011117 (2020). doi:10.1056/NEJMc2011117.

387   16.   Richardson, S. *et al.* Presenting Characteristics, Comorbidities, and Outcomes Among 5700 Patients Hospitalized With COVID-19 in the New York City Area. *JAMA* (2020). doi:10.1001/jama.2020.6775

390   17.   Yu, T-M *et al.* RANTES mediates kidney ischemia reperfusion injury through a possible role of HIF-1α and LncRNA PRINS. Scientific Reports (2016) 10.1038/srep18424

393   18.   Chen, L. Functional roles of CCL5/RANTES in liver disease. Liver Research (2020) 28e34

395   19.   Lescure, F.-X. *et al.* Clinical and virological data of the first cases of COVID-19 in Europe: a case series. *Lancet Infect Dis* (2020). doi:10.1016/S1473-3099(20)30200-0

398   20.   Halama, N., et al. Tumoral immune cell exploitation in colorectal cancer metastases can be targeted effectively by anti-CCR5 therapy in cancer patients. *Cancer Cell* (2016) 29, 587–601, 2016.

401   21.   Grillet, F., Behr, J., Calame, P., Aubry, S. & Delabrousse, E. Acute Pulmonary Embolism Associated with COVID-19 Pneumonia Detected by Pulmonary CT Angiography. *Radiology* 201544 (2020). doi:10.1148/radiol.2020201544

404   22.   Machlus, K. R. *et al.* CCL5 derived from platelets increases megakaryocyte

405   proplatelet formation. *Blood* **127,** 921–926 (2016).

406   23.   Coronavirus survivor credits artificial antibody experimental treatment for

407   recovery. *Los Angeles CBS Local* (2020).

408   https://losangeles.cbslocal.com/2020/04/10/coronavirus-survivor-leronlimab/

409   24.   US National Library of Medicine. Study to Evaluate the Efficacy and Safety of

410   Leronlimab for Mild to Moderate COVID-19. *ClinicalTrials.gov.*

411   https://clinicaltrials.gov/ct2/show/NCT04343651 (2020).

412   25.   US National Library of Medicine. Study to Evaluate the Efficacy and Safety of

413   Leronlimab for Patients With Severe or Critical Coronavirus Disease 2019 (COVID-

414   19). *ClinicalTrials.gov.* https://clinicaltrials.gov/ct2/show/NCT04347239 (2020).

415

| Patient	Age interval/ Gender	Pre-existing conditions	Renal transplant year	Dialysis in hospital	Vasopressors used	Baseline status	Extubated
P1	70-79/M	AKI, HTHD, Prostate CA (s/p prostatectomy), DM, Gout	N/A	Yes	Yes	Intubated	No
P2	70-79/F	ESRD, HTHD, DM, HLD	2018	Yes	Yes	Intubated	No
P3	50-59/M	RF, HTHD, HLD	N/A	Yes	Yes	Venture mask, same day intubated	No
P4	50-59/M	HTHD, Skin CA, Papillary thyroid CA (s/p thyroidectomy), DM	N/A	Yes	Yes	Intubated	Yes
P5	50-59/M	ESRD, CKD stage 3 in renal allograft, recurrent UTI with MDR E.coli, DM, DR, HTHD, HLD	2016	Yes	Yes	Intubated	Yes
P6	40-49/M	FSGS, CKD stage 3, DVT/PE, Gout	2005, 2016	No	No	On 2L NC	N/A
P7	60-69/M	ESRD, Hydronephrosis (s/p stent placement), HTHD, HLD, DM with retinopathy and neuropathy	2018	Yes	Yes	On NRB	Yes
P8	50-59/F	ESRD, lung CA (s/p bilateral upper lobectomy), COPD, Asthma, DM, HTHD, HLD, Hepatitis C	2009	No	No	3-4 L NC*	No
P9	50-59/F	AKI, HTHD, OSA (on Bilevel Positive Airway Pressure)	2006	Yes	Yes	Intubated	No
P10	70-79/M	AKI, CAD, Prostate CA, GERD, HTHD, HLD	N/A	Yes	Yes	Intubated	No

Table 1: Critical COVID-19 Patient Summaries.

N/A = not applicable, s/p = status post-, AKI = acute kidney injury, HTHD = hypertensive heart disease, DM = diabetes mellitus, HLD = hyperlipidemia, ESRD = end-stage renal disease, HD = hemodialysis, CA = cancer, COPD = chronic obstructive pulmonary disease, LUL = left upper lobe, RUL = right upper lobe, MDR = multi-drug resistant, CKD = chronic kidney disease, UTI = urinary tract infection, FSGS = Focal segmental glomerulosclerosis, DVT = deep vein thrombosis, PE = pulmonary embolism, OSA = obstructive sleep apnea, CAD = coronary artery disease, GERD = gastroesophageal reflux disease, RF = renal failure, DR = diabetic retinopathy, NC = nasal canula, NRB = non-rebreather mask, *Patient declined intubation due to poor baseline pulmonary status.
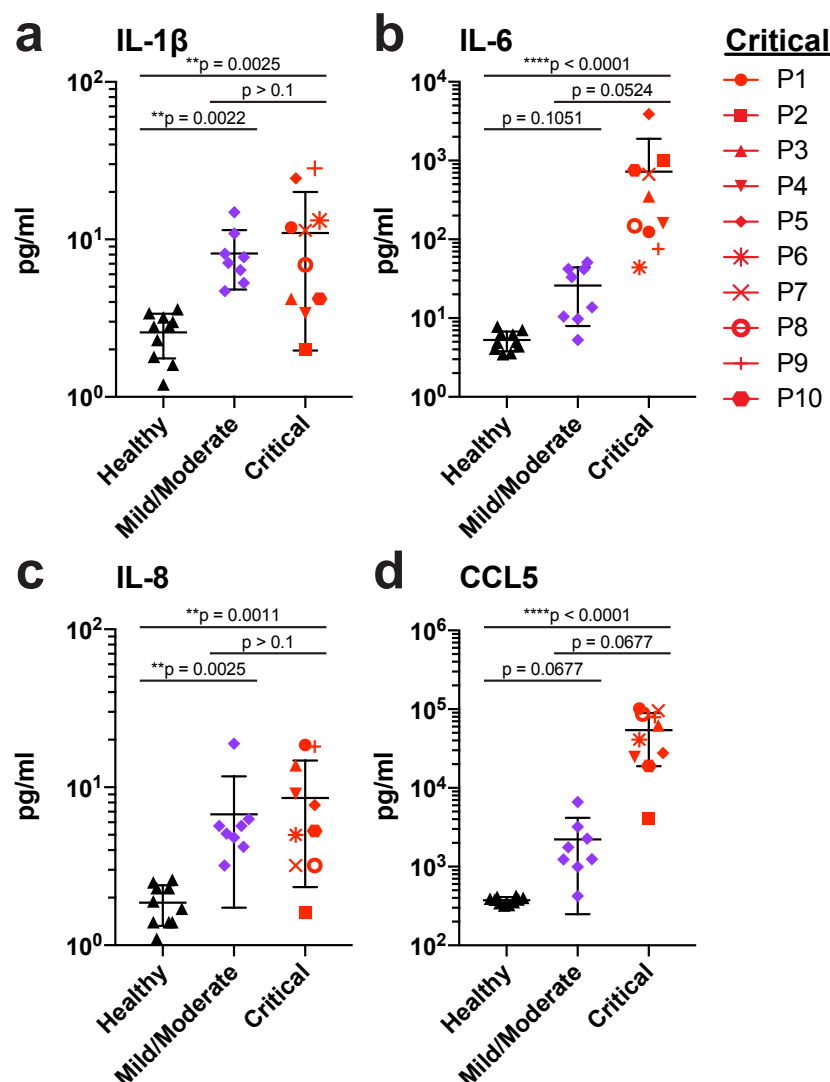
Figure 1. Elevated cytokine and chemokine levels in critically ill COVID-19 patients. a-d, Plasma levels of IL-1β (**a**), IL-6 (**b**), IL-8 (**c**), and CCL5 (**d**) in patients with mild/moderate (n=8, purple symbols) and critical (n=10, red symbols) COVID-19 disease, compared to healthy controls (n=10, black symbols). Graphs display p-values calculated by Dunn's Kruskal-Wallis test: *p ≤ 0.05, ** p ≤ 0.01, ***p ≤ 0.001, ****p ≤ 0.0001.
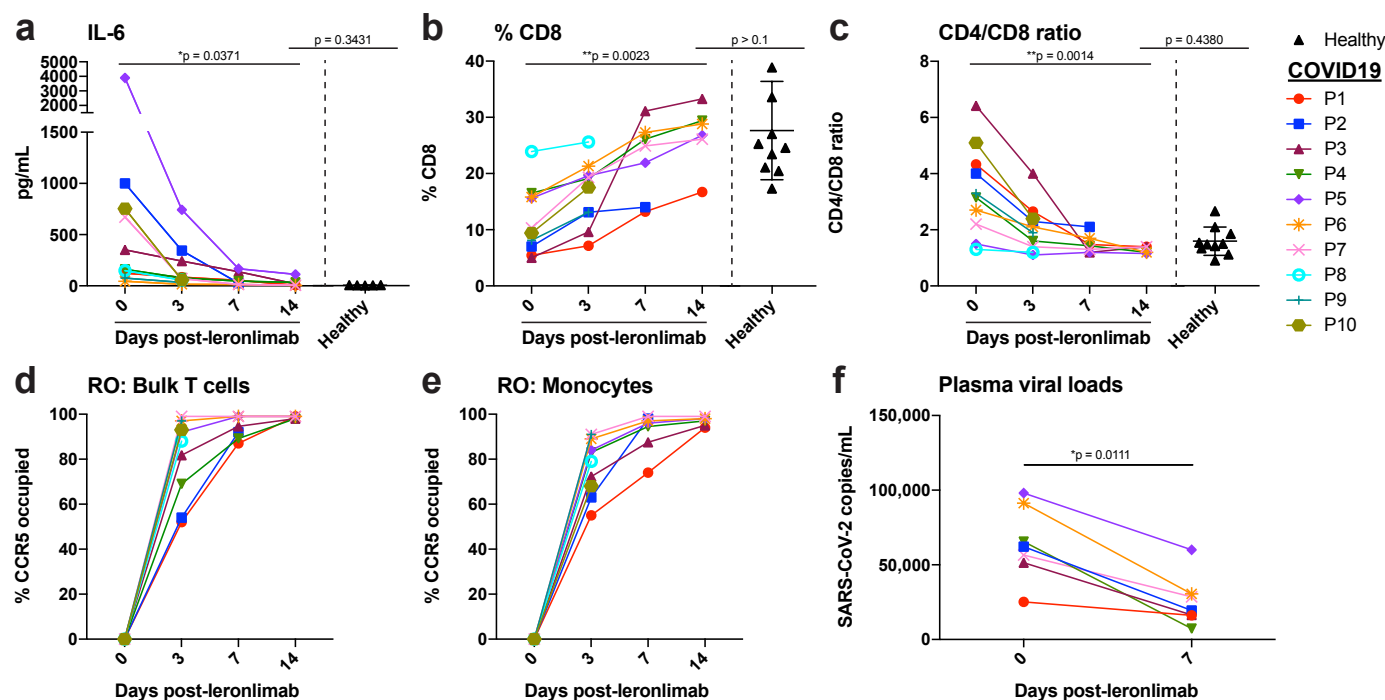
Figure 2. Reversal of immune dysfunction and CCR5 receptor occupancy in critically ill COVID-19 patients after leronlimab administration. a-c, Plasma levels of IL-6 (**a**), and peripheral blood CD8+ T cell percentages of CD3+ cells (**b**) and CD4/CD8 T cell ratio (**c**) at days 0 (n=10), 3 (n=10), 7 (n=7), and 14 (n=6) post-leronlimab administration. Healthy controls (n=10) shown in black triangles. Graphs display p-values calculated by Dunn's Kruskal-Wallis test: not significant p > 0.05, *p ≤ 0.05, ** p ≤ 0.01, ***p ≤ 0.001, ****p ≤ 0.0001. **d-e,** CCR5 receptor occupancy on peripheral blood bulk T cells (**d**), and monocytes (**e**). **f,** SARS-CoV-2 plasma viral load at days 0 and 7 post-leronlimab (n=7). Graph displays p-value calculated by Mann-Whitney test: *p ≤ 0.05, ** p ≤ 0.01, ***p ≤ 0.001, ****p ≤ 0.0001.
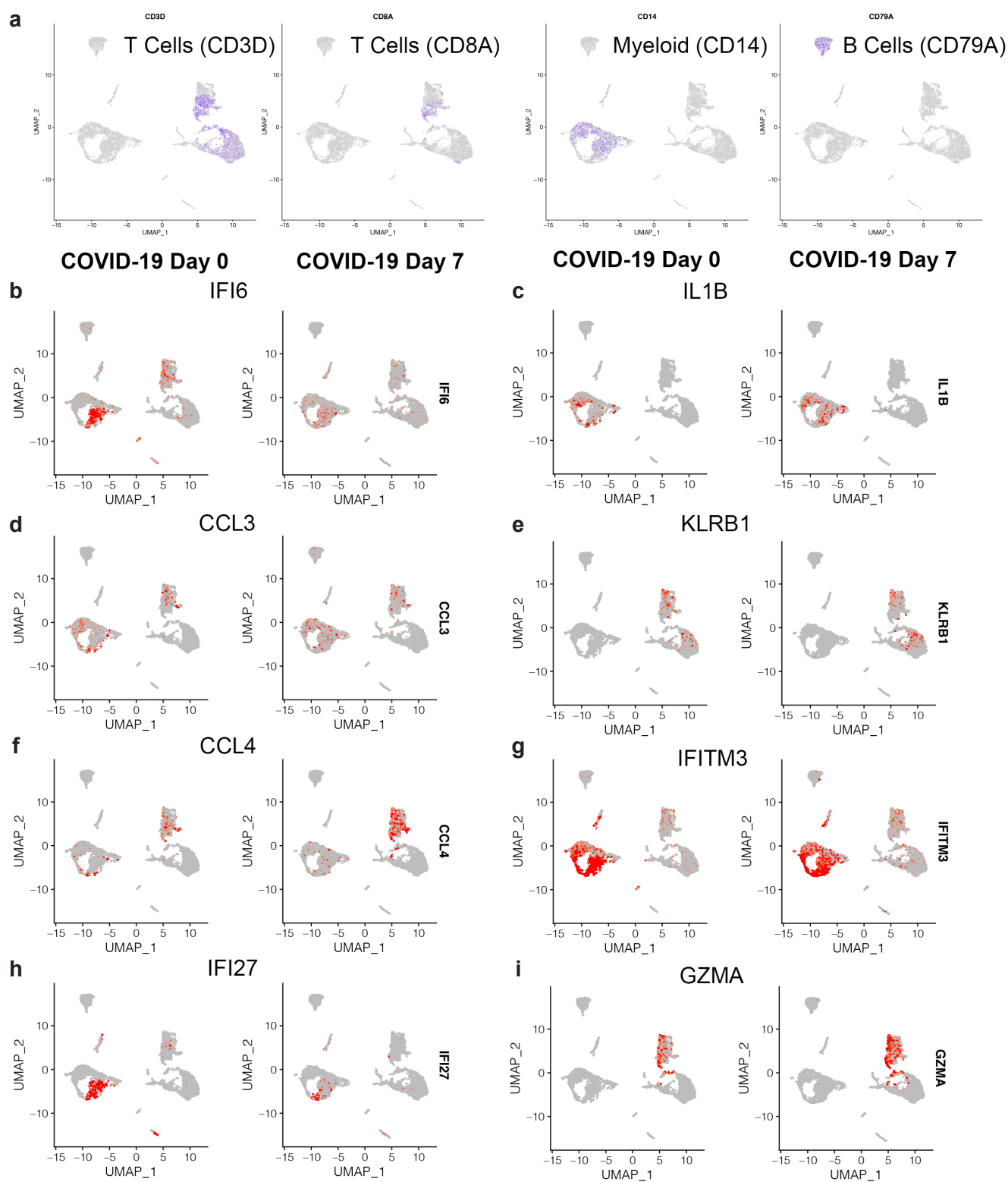
Figure 3. Longitudinal single-cell transcriptomics of COVID-19 following leronlimab.

UMAP feature plots of single-cell transcriptome profiles of CD3 (T cells) versus CD8 (CD8+ T cells) versus CD14 (monocyte/myeloid) versus CD79a (B cells) (**a**) IFI6 (**b**), IL-1β (**c**), CCL3 (**d**), KLRB1 (**e**), CCL4 (**f**), IFITM3 (**g**), IFI27 (**h**), Granzyme A (**i**), before and 7 days post leronlimab treatment for severe COVID-19 patients P2 and P4.